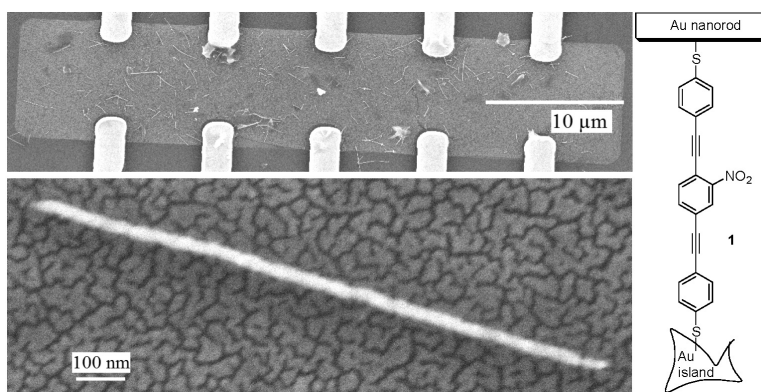Article

NanoCell Electronic Memories

James M. Tour, Long Cheng, David P. Nackashi, Yuxing Yao, Austen
K. Flatt, Sarah K. St. Angelo, Thomas E. Mallouk, and Paul D. Franzon

More About This Article

Additional resources and features associated with this article are available within the HTML version:

- Supporting Information
- Links to the 12 articles that cite this article, as of the time of this article download
- Access to high resolution figures
- Links to articles and content related to this article
- Copyright permission to reproduce figures and/or text from this article

View the Full Text HTML

NanoCell Electronic Memories

James M. Tour,*,† Long Cheng,† David P. Nackashi,‡ Yuxing Yao,† Austen K. Flatt,†
Sarah K. St. Angelo,§ Thomas E. Mallouk,*,§ and Paul D. Franzon*,‡

*Contribution from the Departments of Chemistry and Computer Science, Center for
Nanoscale Science and Technology, Rice University, Houston, Texas 77005,
Department of Electrical and Computer Engineering, North Carolina State University,
Raleigh, North Carolina 27695, and Department of Chemistry,
The Pennsylvania State University, University Park, Pennsylvania 16802*

Received May 27, 2003; E-mail: tour@rice.edu

Abstract: NanoCells are disordered arrays of metallic islands that are interlinked with molecules between micrometer-sized metallic input/output leads. In the past, simulations had been conducted showing that the NanoCells may function as both memory and logic devices that are programmable postfabrication. Reported here is the first assembly of a NanoCell with disordered arrays of molecules and Au islands. The assembled NanoCells exhibit reproducible switching behavior and two types of memory effects at room temperature. The switch-type memory is characteristic of a destructive read, while the conductivity-type memory features a nondestructive read. Both types of memory effects are stable for more than a week at room temperature, and bit level ratios (0:1) of the conductivity-type memory have been observed to be as high as 10^4:1 and reaching 10^6:1 upon ozone treatment, which likely destroys extraneous leakage pathways. Both molecular electronic and nanofilamentary metal switching mechanisms have been considered, though the evidence points more strongly toward the latter. The approach here demonstrates the efficacy of a disordered nanoscale array for high-yielding switching and memory while mitigating the arduous task of nanoscale patterning.

Nanoelectronic architectures could prove to be a complement to traditional solid-state devices.[1–3] Most proposed architectures are dependent upon precise order and on building devices with exact arrays of nanostructures (i.e., molecule-embedded crossbars) painstakingly interfaced with microstructure.[4–8] Conversely, the NanoCell approach, as previously described and simulated,[1,9] is not dependent on placing molecules or nanosized metallic components in precise orientations or locations. The internal portions are, for the most part, disordered and there is no need to precisely locate any of the switching elements. The nanosized switches are added in abundance between the micrometer-sized input/output electrodes, and only a small percentage of them need to assemble in an orientation suitable for switching. The result of the NanoCell architecture is that the patterning challenges of the input/output structures become far less exacting since standard micrometer-scale lithography can afford the needed address system. Also, fault tolerance is enormous.[9] However, programming is significantly more challenging than when ordered ensembles are used. This paper describes the first example in which a NanoCell is actually assembled. Remarkably, the NanoCell exhibits reproducible switching behavior with excellent peak-to-valley (PVR) ratios,[10] peak currents in the milliamp range, and reprogrammable memory states that are stable for more than a week with substantial 0:1 bit level ratios.

A NanoCell is a two-dimensional unit of juxtaposed electrodes fabricated atop a Si/SiO$_2$ substrate.[1] In the embodiment described here, five Au electrode pairs were patterned on opposing sides of the NanoCell (Figure 1, top). A discontinuous gold film was vapor-deposited onto the SiO$_2$ in the central region (Figure 1, bottom). The chips were always treated with UV-ozone and ethanol-washed immediately prior to use in order to remove exogenous organics. Electrical measurements confirm the absence of DC conduction paths across the discontinuous Au film between the five juxtaposed pairs of ~5 μm-spaced

† Rice University.
‡ North Carolina State University.
§ The Pennsylvania State University.

(1) Tour, J. M. *Molecular Electronics: Commercial Insights, Chemistry, Devices, Architecture and Programming*; World Scientific: Teaneck, NJ, 2003.
(2) Tour, J. M. *Acc. Chem. Res.* **2000**, *33*, 791.
(3) (a) Carroll, R. L.; Gorman, C. B. *Angew. Chem., Int. Ed.* **2002**, *41*, 4378–4400. (b) Goldhaber-Gordon, D.; Montemerlo, M. S.; Love, J. C.; Opiteck, G. J.; Ellenbogen, J. C. *Proc. IEEE* **1997**, *85* (4), 521–540.
(4) Heath, J. R.; Kuekes, P. J.; Snider, G. S.; Williams, R. S. *Science* **1998**, *280*, 1716.
(5) Lent, C. S.; Tougaw, P. D. *Proc. IEEE* **1997**, *85*, 541–557.
(6) Goldstein, S. C.; Budiu, M. *Proc. ISCA* **2001**, 178–191.
(7) Melosh, N. A.; Boukai, A.; Diana, F.; Geradot, B.; Badoloato, A.; Petrof, P. M.; Heath, J. R. *Science* **2003**, *300*, 112–115.
(8) Huang, Y.; Duan, X.; Cui, Y.; Lauhon, L. J.; Kim, K.-H.; Lieber, C. M. *Science* **2001**, *294*, 1313.
(9) Tour, J. M.; Van Zandt, W. L.; Husband, C. P.; Husband, S. M.; Wilson, L. S.; Franzon, P. D.; Nackashi, D. P. *IEEE Trans. Nanotechnol.* **2002**, *1*, 100.
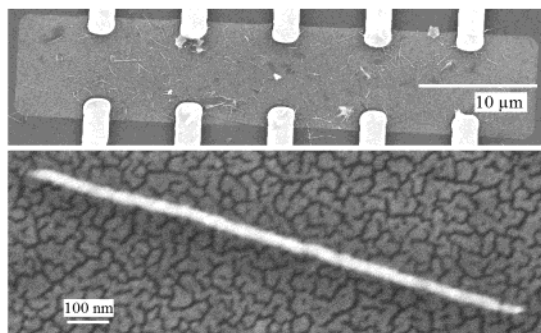(10) Chen, J.; Reed, M. A.; Rawlett, A. M.; Tour, J. M. *Science* **1999**, *286*, 1550.

Figure 1. SEM image of the NanoCell after assembly of the Au nanowires and **1**. The top image shows the five juxtaposed pairs of fabricated leads across the NanoCell, and some Au nanowires are barely visible on the internal rectangle of the discontinuous Au film. The lower image is a higher magnification of the NanoCell's central portion showing the disordered discontinuous Au film with an attached Au nanowire, which is affixed via the OPE-dithiol (not observable) derived from **1**.

electrodes (≤1 picoamp up to 30 V). In this study, each juxtaposed pair serves as an independent memory bit address system.

1
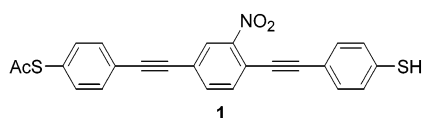
The assembly of molecules and nanowires in the central portion of the NanoCell was then carried out, under N_2, to provide a current pathway across the NanoCell. Compounds similar to the mononitro oligo(phenylene ethynylene) (OPE), **1**,[11] have been shown previously to exhibit switching and memory storage effects when fixed between proximal Au probes.[10,12] Au nanowires (30 nm diameter and 300−2000 nm long, grown in a polycarbonate membrane by electrochemical reduction at 1.2 C)[13] were added to a vial containing **1** (0.8 mg) in CH_2Cl_2 (3 mL). The vial was agitated (platform auto shaker, 250 rpm) for 40 min to dissolve the polycarbonate membrane and to form **1**-encapsulated Au nanowires via chemisorption of the thiols to the nanowires.[14] Because the thiol groups are far more reactive toward Au than thioacetyl groups,[15] this procedure leaves the latter projecting away from the nanowire surfaces.[16] NH_4OH (5 μL, concentrated) and ethanol (0.5 mL) were added and the vial was agitated for 10 min to

(11) Compound **1** was prepared by the formation of the α-thiolacetate ω-thiol-*tert*-butoxycarbonyl. The latter was removed with TFA without disruption of the thiolacetate. A manuscript (Flatt, A. K.; Yao, Y.; Maya, F.; Tour, J. M.) is in preparation detailing this orthogonal deprotection approach.
(12) Chen, J.; Wang, W.; Reed, M. A.; Rawlett, A. M.; Price, D. W.; Tour, J. M. *Appl. Phys. Lett.* **2000**, *77*, 1224.
(13) Mbindyo, J. K. N.; Mallouk, T. E.; Mattzela, J. B.; Kratochvilova, I.; Razavi, B.; Jackson, T. N.; Mayer, T. S. *J. Am. Chem. Soc.* **2002**, *124*, 4020.
(14) Assemblies of thiols on Au nanorods have been studied. See, for example, (a) Martin, B. R.; Dermody, D. J.; Reiss, B. D.; Fang, M.; Lyon, L. A.; Natan, M. J.; Mallouk, T. E. *Adv. Mater.* **1999**, *11*, 1021−1025. (b) Martin, B. R.; St. Angelo, S. K.; Mallouk, T. E. *Adv. Funct. Mater.* **2002**, *12*, 759.
(15) Tour, J. M.; Jones, L., II; Pearson, D. L.; Lamba, J. S.; Burgin, T. P.; Whitesides, G. W.; Allara, D. L.; Parikh, A. N.; Atre, S. *J. Am. Chem. Soc.* **1995**, *117*, 9529.
(16) This was further verified by the assembly of **1** on a surface of freshly deposited Au (on Cr/Si) for 24 h, in the absence and presence of polycarbonate, and checking by ellipsometry after rinsing the surface well. Ellipsometric thicknesses were consistent with near-monolayer formation of **1**: 2.8 ± 0.25 nm in the absence of polycarbonate (calcd 2.5 nm excluding the tilt[15] from the surface normal) and 3.1 ± 0.25 nm in the presence of polycarbonate. Therefore, as expected,[14] polycarbonate did not affect the SAM formation; however, a small amount of multilayer formation was occurring, presumably due to loss of the acetate and disulfide formation over the prolonged assembly time.[15]
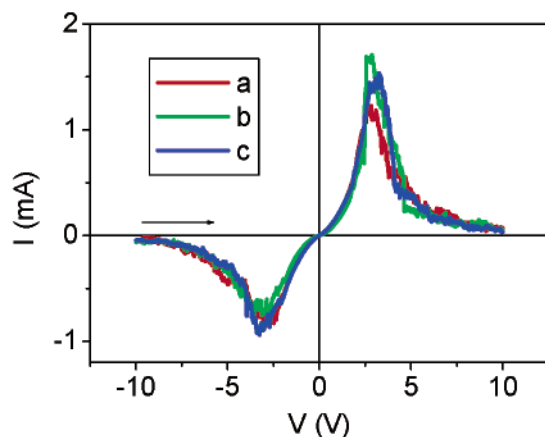
Figure 2. $I(V)$ characteristics of the NanoCell at 297 K. Curves a, b, and c are the first, second, and third sweeps, respectively (∼40 s/scan). The PVRs in curve c are 23:1 and 32:1 for the negative and positive switching peaks, respectively. The black arrow indicates the sweep direction of negative to positive.

remove the acetyl group.[17] A chip containing 10 NanoCell structures was placed in the vial (active side up), and the vial was further agitated for 27 h to permit the nanowires to interlink the discontinuous Au film via the OPEs (Figure 1). The chip was removed, rinsed with acetone, and gently blown dry with N_2.

The assembled NanoCells were electrically tested on a probe station (Desert Cryogenics, TTProber 4) with a semiconductor parameter analyzer (Agilent 4155C) at room temperature (297 K) under vacuum (10^{-5} mmHg). Typical $I(V)$ characteristics of the NanoCell devices are shown in Figure 2. Two stable and reproducible switching peaks are observed in a bias range of −10 and +10 V. It is expectedly asymmetric because the molecule, due to the nitro-group orientation, is asymmetrically oriented, and/or the contacts are likely slightly different on each end. After about 300 scans, the switching responses further stabilized in peak voltage; the device showed no degradation to >2000 scans over a 22 h period of continuous sweeping. Also, after testing, an assembled NanoCell was stored in a capped vial (air) for 2 months with little, if any, signal variations relative to the readings recorded at the initial testing.

A juxtaposed pair of electrodes, as described above, showed little variation in its behavior over several thousand scans. However, there were notable differences when different electrode pairs were compared, in that they showed variations in peak current position (occurring typically in a range of 3−15 V), peak current (typically 0.1−1.7 mA), and PVR (typically 5−30). The differences are undoubtedly related to the variations in the conduction pathways of these disordered arrays.

If a voltage sweep is conducted on a NanoCell in a bias range that is up to or not far beyond the peak of the $I(V)$ curve (switching event), a pseudolinear trace is observed, as shown by curve a (0 state) in Figure 3. However, if three voltage pulses at −8 V (100 ms width, 104 ms period) are then applied to the same pair of leads, a peak appears (1 state) in the first scan after the voltage pulses, as shown by curve b in Figure 3. Apparently the voltage pulses set the system into a new state that is then read by the bias sweep b. This is being termed the switch-type memory effect. The following scans c and d,

(17) Cai, L.; Yao, Y.; Yang, J.; Price, D. W., Jr.; Tour, J. M. *Chem. Mater.* **2002**, *14*, 2905.
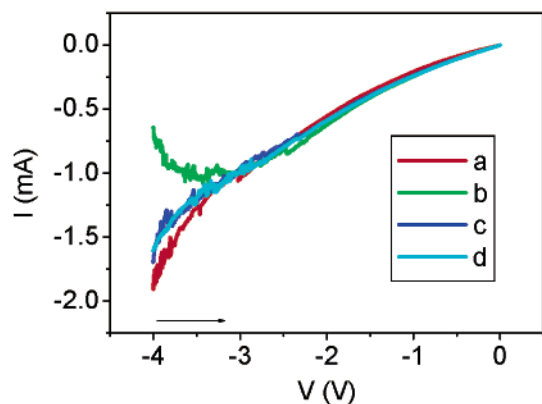
Figure 3. *I*(*V*) characteristics of the NanoCell before (a) and after (b−d) three voltage pulses at −8 V at 297 K. Curves b, c, and d were the first, second, and third scans (after the −8 V reset pulses), respectively. Scans a−d were run at ∼40 s/scan. The results here are from the same device used to generate the *I*(*V*) curve in Figure 2.

Figure 4. *I*(*V*) characteristics of the NanoCell before (scans a−c) and after (scans d−f) three voltage set-pulses of −8 V at 297 K. The initial high-σ state (0 state) is represented by curves a, b, and c, which are the first, second, and third scans before the set-pulse, respectively. The low-σ state (1 state) is represented by curves d, e, and f, which are the first, second, and third scans after the −8 V set-pulses, respectively. The inset shows scans d−f in the microamp range. Scans a−c were run at ∼40 s/scan; scans d−f were run at ∼50 s/scan. This is the same device as depicted in Figures 2 and 3.

however, produced *I*(*V*) responses similar to curve a, the scans before the voltage pulses, suggesting that the state set by the voltage pulse was erased after it was read by scan b. In other words, the switch-type memory effect has a destructive-read property (as seen with present-day DRAM). A positive voltage pulse, i.e., +8 V, can also set the system into the 1 state. Voltages higher than ±8 V always worked, but voltages lower than ±8 V did not set this particular NanoCell into the 1 state. All of the active NanoCells showed this rewritable behavior, although the magnitudes and set voltages varied between different NanoCells as described above.

On the same device as shown in Figures 2 and 3, another type of memory effect was found that has a nondestructive-read, the so-called conductivity-type memory, which operates by the storage of a high- or low-conductivity (σ) state. The difference between the switch-type memory and the conductivity-type memory is based upon the voltage-sweep range, namely, −4 to 0 V for the former and −2 to 0 V for the latter. An initially high conductivity state (high-σ or 0 state) was observed in a bias range of −2 to 0 V as shown in Figure 4, curves a−c. The high-σ state is changed (written) into a low-σ state (1 state) upon application of three voltage pulses at −8 V (100 ms width, 104 ms period), as shown by curves d−f. The low-σ state persists as a stored bit, which is essentially unaffected by successive read sweeps. There is a 400:1 0-state:1-state ratio in current levels between the high- and low-σ states recorded at −2 V for this NanoCell device. The ratios may vary between different electrode pairs but the ratio here is representative. The highest observed 0:1 ratio was 12 500:1 (198 μA:16 nA at −2.0 V) for a 5-μm gap electrode pair, and the lowest observed ratio was 10:1 at the same voltage.

The conductivity-type memory effect is independent of bias sweep directions. Once set into the low-σ state upon application of voltage-set (write) pulses, the system holds the low-σ state regardless of negative bias sweep from 0 to −2 V or positive bias sweep from 0 to 2 V. Several routes were investigated to erase the stored low-σ state (written bit). Voltage pulses at −3 to −4 V (∼20 pulses at 1 ms pulse width, 10 ms pulse period) reset the memory into the original high-σ state (use a voltage pulse that comes near the peak of the switching event but not far past the peak). Although the read, write and erase signal conditions were accurately characterized with the parameter
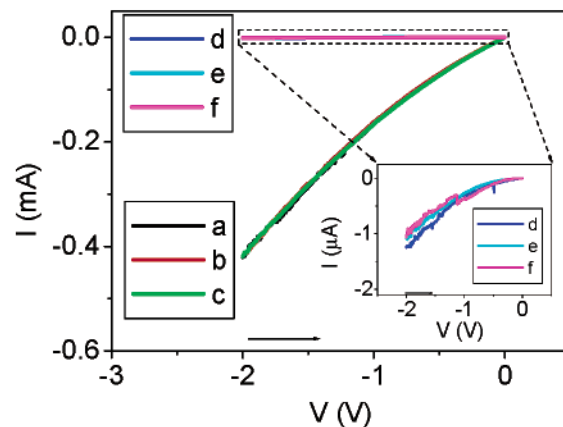
analyzer, precise memory access and switching times will be investigated with a separate high-speed instrument. Millisecond, or faster, switch times might be possible with smaller structures where the wire delays are kept to a minimum. The switch-type and conductivity-type memory effects are shown here in the negative bias regions; however, they apply in positive bias region as well.

The bit retention time for the switch-type memory is at least 11 days and with ∼10% change in the voltage peak position of the curves when compared to the read tests run seconds after the written state was set; however, there was no decline in the magnitude of the response. The conductivity-type memory persisted for at least 9 days. Over this period, the 0:1 signal magnitudes interestingly increased, although the reset voltages also drifted higher (∼10%) over this period. Therefore, the two types of memory effects can have much longer retention times, but these are merely the time periods over which they have been tested. Longer durations were not studied. During waiting periods over which these retention times were recorded, the NanoCells had been occasionally exposed to air (1 atm), for periods of up to 30 min, as more samples were moved through the testing chamber. Therefore, the stored written states are robust even with short exposure to air.

Yields of functioning NanoCells that have been prepared by the protocol described here seemed to be electrode gap-dependent. A thus-prepared NanoCell chip showed 100%, 65%, and 30% yields for devices with 5, 10, and 20 μm spacings between the juxtaposed electrodes, respectively.

The assembled chips were tested in the probe station both in the dark (covering the observation window with aluminum foil) and in the presence of the room light with the station's fiber optic observation light projected through the observation window ∼10 cm above the chip. The same electrical responses were obtained regardless of the lighting, thereby excluding a photo-conductive mechanism.

Several control experiments were conducted in order to investigate the mechanism of action for the NanoCell memories. When the same assembly process was conducted but **1** was not added (only Au nanowires in polycarbonate, CH_2Cl_2, NH_4OH,

and ethanol were added), all the leads were "open" and no switching behavior was observed over the tested 15 juxtaposed electrodes (5 pairs at 5 μm spacings, 5 pairs at 10 μm spacings, and 5 pairs at 20 μm spacings). Therefore, the process is **1**-dependent. When the assembly procedure was conducted but the nanowires were not present (only **1**, polycarbonate devoid of nanowires, CH_2Cl_2, NH_4OH, and ethanol were added), two out of three juxtaposed 5 μm spacings showed switching between them; however, the switching effect signal degraded nearly completely after 3−10 scans. Therefore, some molecules may have bridged the discontinuous Au film, but the connections were not as abundant or stable. A similar behavior was observed at 10 μm spacings between the electrodes. When an alkyl system, $AcS(CH_2)_{12}SH$ (**2**),[18] was substituted for **1** in the standard assembly process, and 30 juxtaposed electrode pairs were studied, 28 showed no device behavior. Interestingly, however, one 5 μm electrode pair showed the characteristic switching that dissipated after three scans, while a second electrode pair showed reproducible switching behavior but the onset and peak currents occurred at 14 V. Therefore **1** is not unique among molecule types.

Concerning the mechanism underlying the programmable memories, a molecular electronic effect was first considered. Several mechanisms have been proposed for molecular electronic switching.[19−21] They are based upon charging of the molecules, which results in changes in the contiguous structure of the lowest unoccupied molecular orbital (LUMO). This can further be accompanied by conformational changes that would modulate the current based on changes in the extended π-overlap. As the voltage is increased, the molecules in discrete nanodomains would enter into differing electronic states. Conversely, as some have pointed out, so-called molecular-based switching might not be an inherently molecular phenomenon, but it results from surface bonding rearrangements that are molecule/metal contact in origin (i.e., a sulfur atom changing its hybridization state, or more simply, subangstrom shifts between different Au surface atom bonding modes or molecular tilting).[22,23] An estimate of the number of molecular junctions between a set of juxtaposed electrode pairs is difficult to gauge; however, on the basis of the size of the nanowires and the Au islands (which can be 0.3−1 μm long), the number of molecular junctions could be as few as four in a 5 μm electrode gap. The number of molecules in parallel, per junction, could be as few as 30 or as many as several thousand, based on the nanowire diameters and lengths. Note that the quantum conductance of each molecule is ∼0.08 mA/V.

In addition to a molecular electronic process, electromigration was considered as a cause for the high currents and

reset operations that are analogous to filamentary metal memories.[24−27] To further investigate this point, the exposed organic material was stripped from a working NanoCell by treating the assembled chip with UV-ozone for 10−30 min. Remarkably, the device behavior of the NanoCell remained and often improved. In some cases, the 0:1 bit level ratios for the conductivity memory even increased up to 10^6:1 (2.53 mA:0.76 nA at −3.0 V). This could suggest that the ozone was not able to penetrate through the build-up of the oxidatively destroyed organics in order to reach the small amount of active organic molecules in the key nanodomains that are sandwiched between the nanowires and the Au islands and that the more exposed leakage routes were destroyed by the ozone. Conversely, it could suggest that indeed filamentary metal had grown along the molecules and that these metal filaments were causing the observed switching behavior, with any molecular leakage routes being destroyed by the ozone. It was previously shown, by modeling, that the NanoCell should exhibit extraordinary resistance to degradation (defect tolerance) due to the abundance of molecules available for switching; furthermore, if one molecule degrades, another could slip into place from the self-assembled monolayers that cover all the surrounding metal surfaces.[9] Consider also that, at the atomistic level, a molecular change in either conformation or hybridization at the metal−molecule interface, due to voltage changes or charging, could give electronic response characteristics that are analogous to filamentary metals (atoms moving in and out of alignment for current flow), and thereby resemble negative differential resistance-like behavior.[10] In other words, metallic nanofilaments could form during a voltage sweep, then on increasing the voltage, they could exhibit a sudden break, causing a decline in the current.[27]

Additionally, a mechanical motion involving the molecule-covered nanowires was considered. However, it was deemed less likely due to the highly cross-linked nature of the micrometer-sized matrix.

None of the former data was conclusive enough to exclude either the molecular electronic-based mechanism or the nanofilament mechanism. However, a later finding pointed toward the nanofilament-based mechanism being the dominant or exclusive pathway. As described above, we had never seen the switchlike behavior from the bare chips; they just showed open circuits. As customary to ensure open circuits before we began the molecule/nanowire assembly, while probing an older chip (4 months storage at room temperature in a Fluoroware container) from the same lot of chips that was used to prepare the NanoCell described here, we noticed switching with magnitudes similar to the levels outlined in Figure 2. Neither nanowires nor molecules had been added;[28] it was merely the aged discontinuous Au film vapor-deposited between electrodes. Possibly, while the film had aged, the islands migrated across the gaps sufficiently close together to form nanofilaments upon voltage scanning, and then metal filament breakage occurred at higher voltages, giving responses similar to that shown in

(18) Compound **2** has been prepared previously. See Bain, C. D.; Troughton, E. B.; Tao, Y.-T.; Evall, J.; Whitesides, G. M.; Nuzzo, R. G. *J. Am. Chem. Soc.* **1989**, *111*, 321. Note that **2** is ∼1 Å shorter in length than **1**; however, the effective length of **2** will be ∼3−4 Å shorter since alkanethiols have ∼33° tilt from the surface normal (resulting in 1.8 nm Au-to-acetate distance) while the OPEs have <20° tilt.[15]

(19) Seminario, J. M.; Derosa, P. A.; Bastos, J. L. *J. Am. Chem. Soc.* **2002**, *124*, 10266−10267.

(20) Cornil, J.; Karzazi, Y.; Bredas, J. L. *J. Am. Chem. Soc.* **2002**, *124*, 3516−3517.

(21) Fan, F.-R. F.; Yang, J.; Cai, L.; Price, D. W.; Dirk, S. M.; Kosynkin, D.; Yao, Y.; Rawlett, A. M.; Tour, J. M.; Bard, A. J. *J. Am. Chem. Soc.* **2002**, *124*, 5550.

(22) Donhauser, Z. J.; Mantooth, B. A.; Kelly, K. F.; Bumm, L. A.; Monnell, J. D.; Stapleton, J. J.; Price, D. W., Jr.; Rawlett, A. M.; Allara, D. L.; Tour, J. M.; Weiss, P. S. *Science* **2001**, *292*, 2303.

(23) Rawlett, A. M.; Hopson, T. J.; Nagahara, L. A.; Tsui, R. K.; Ramachandran, G. K.; Lindsay, S. M. *Appl. Phys. Lett.* **2002**, *81*, 3043.

(24) Buckley, W. D. U.S. Patent 3,980,505, September 14, 1976.

(25) Chesnys, S.-A.; Karpinskas, A. U. *Technol. Phys.* **2002**, *47*, 58.

(26) Simmons, J. G.; Verderber, R. R. *Proc. R. Soc. London, Ser. A, Math Phys. Sci.* **1967**, *301*, 77.

(27) Thurstans, R. E.; Oxley, D. P. *J. Phys. D: Appl. Phys.* **2002**, *35*, 802.

(28) There may have been adventitious airborne molecules assembled between the metallic islands; however, we always treated the chips with UV ozone prior to use. Therefore, their presence is unlikely to be a significant factor.

Figure 2.[27] The metallic island migration was not obvious by microscopic analysis of the discontinuous Au films because the resolution needed within the topologically nonplanar arrays cannot be achieved with either scanning electron (SEM) or atomic force (AFM) microscopy. We carried out $I(V,T)$ (current as a function of voltage and temperature, -2 to 2 V, 280 to 80 K and back to 280 K) measurements to assess the possible conduction mechanism of the high-σ conductivity-type memory state on the bare chip. The data suggested "dirty" or modified-metal conduction:[26] metallic conduction with trace impurities.[28] The same type of $I(V,T)$ measurements on a molecule/nanowire assembled NanoCell showed both a temperature dependence and a nontemperature dependence based on the particular juxtaposed electrode set studied. Albeit confusing, there may be a duality of mechanisms coexisting on the same chip. Further studies are ongoing to better discern this process. Therefore, although we cannot rule out a molecular electronic mechanism for the NanoCells, based on the latest observation carried out on aged but bare arrays, the data are suggestive of a nanofilamentary metal mechanism in some cases.[26,27]

In conclusion, a NanoCell assembled with disordered arrays of molecules and nanowires is presented. The NanoCell exhibits reproducible switching behavior and two types of memory effects, one being a destructive read and the second a non-destructive read. Both types of memories are stable for over a week at room temperature and probably much longer. Data suggest that nanofilamentary metal formation is the likely mode of current transport, but fabrication of NanoCells with more refractory metals such as Pt or Pd will be carried out to further test this point. Additionally, we are currently making chips with a 193 nm stepper to yield juxtaposed electrode gap spacings of <1 μm with smaller Au-film islands and appropriately sized nanowires, with the hope of attaining higher degrees of consistency between electrode pairs. With the presently sized embodiments, write/erase speeds, and the lack of isolation and fanout, the NanoCell is not a harbinger for DRAM, flash, or MRAM replacements. However, it demonstrates the first fabrication of a disordered nanoscale ensemble for high-yielding switching and memory while mitigating the painstaking task of nanoscale lithography or patterning, thereby furthering the promise of disordered programmable arrays for complex device functionality.[1,9]

JA036369G